

## Research Article

# Influence of Concrete Compressive Strength on CFRP Strengthening and Repairing of RC Two-Way Slabs

Mohammed F. Ojaimi , Meyyada Y. Alabdulhady , and Kadhim Z. Naser 

*Department of Civil Engineering, College of Engineering, University of Basrah, Basrah, Iraq*

Correspondence should be addressed to Kadhim Z. Naser; [kadhimzuboon@gmail.com](mailto:kadhimzuboon@gmail.com)

Received 4 November 2023; Revised 10 April 2024; Accepted 7 June 2024

Academic Editor: Mohamed Moafak Arbili

Copyright © 2024 Mohammed F. Ojaimi et al. This is an open access article distributed under the Creative Commons Attribution License, which permits unrestricted use, distribution, and reproduction in any medium, provided the original work is properly cited.

In this research, the feasibility of strengthening and repairing two-way reinforced concrete slabs and the effect of compressive strength on the properties of strengthened and repaired slabs using CFRP sheets were studied. The experimental program includes testing twelve samples. Four samples served as control panels, while four samples were strengthened using CFRP sheets to study the effect of carbon sheets on the ultimate load capacity. Also, the four pretested control panels were also taken and rerepaired using CFRP sheets and retested for the purpose of evaluating their properties after repair. The ultimate load capacity, energy dissipation capacity, initial stiffness, and failure pattern were explained by the experimental results obtained. The experimental results revealed that the use of CFRP strips led to an improvement in the average ultimate loading capacity by 16.2% and 6.45% for the strengthening and repairing system, respectively. Also, the utilization of the CFRP strips as a strengthening system significantly improved the stiffness and the cracking load of RC two-way slabs. It was also noted that the ultimate loading capacity was proportionally related to the concrete strength for strengthened slabs with an increase of 23.3% for slabs with the highest concrete strength (C: 70).

## 1. Introduction

Many structures built in the past are currently considered unsafe, and some of their members need to be strengthened or repaired. The need to strengthen structural members in constructed buildings comes because of errors in the design, flaws in the implementation, changes in the structure use, changes in the applied load, and increase in design requirements according to the design codes. There is a need to repair the reinforced concrete structural elements in buildings and bridges because they are prone to lose some of their structural function during their service life due to various factors, including weather deterioration, exposure to loads more than the design loads, earthquakes, and so on [1–4].

The service life of the engineering structures highly depends on the climatic conditions surrounding the structure during its service period. The mechanical properties of the concrete are changed due to the harmful

chemical reactions in the concrete exposed to environmental conditions. One of the most important and dangerous challenges facing the planet Earth is climate change, which greatly affects the sustainability of engineering facilities. Human activities on planet Earth are considered one of the most important causes of climate change. Increasing the service life of the structures has a significant positive impact on the climate conditions by reducing the need for energy and raw material consumption [5]. The current study contributes to increase the service life of concrete structures by strengthening or repairing the two-way slab.

Consequently, several techniques were investigated to overcome these degradations and/or improve the functions of different structural elements such as slabs, beams, and columns. Mainly, these techniques were used to increase the load-carrying capacity. Such methods are section enlargement, externally bonded steel plates, fiber-reinforced polymers (FRPs), near-surface mounted, and so on [6–12]. However, a large number of studies were found on using

FRP composite as an effective strengthening or repairing system owing to its properties including high tensile strength, lightweight, excellent corrosion resistance, fatigue resistance, nonmagnetic material, and thermal insulation [13–15].

Recently, plenty of studies have been conducted on the efficiency of using FRP as an external reinforcement to boost the strength of RC one-way slabs [16–25] or RC two-way slabs [26–40]. The most important factors that were investigated in the previous studies are the different FRP composite systems, internal and external reinforcement ratios, slab shape (i.e., circle, square, and rectangular), and loading type. However, no studies are available on the influence of varying concrete compressive strength on the flexural overall behavior of RC two-way slabs. Furthermore, the available studies on the behavior of RC two-way slabs without opening under monotonic loading conditions are quite limited. For instance, Limam et al. [26] investigated the implication of adding the CFRP strips as a strengthening material on the tension face of RC two-way slabs. The results revealed that CFRP can be efficiently used as a strengthening material. Furthermore, good agreement was found between theoretical and experimental results. Mosallam and Mosallam [27] evaluated experimentally the ultimate and overall behavior response of RC two-way slabs strengthened using CFRP and GFRP strips. The improvement in the ultimate capacity was around 200% which indicated that the CFRP system was efficiently suitable for flexural strengthening of RC two-way slabs. The experimental results were also compared to the numerical simulation with a positive correlation being found between them. Ebead and Marzouk [28] conducted experimentally the implementation of a layer strip of CFRP and GFRP as a strengthening system at the tension side of RC two-way slabs with a low internal reinforcement ratio of 0.35% and 0.5%. Results showed that the ultimate capacity of two-way slabs using CFRP strips could be increased up to 35% over the reference specimen. Chen et al. [31] examined the use of different FRP composite materials (i.e., CFRP, GFRP, and BFRP) as a strengthening system of RC two-way slabs. The outcomes showed that the CFRP system was preferable as compared to other FRP materials. Therefore, more investigations are required to extend the knowledge on the flexural overall behavior of RC two-way slabs without opening strengthening or repairing system with CFRP composite and to explore more factors that influence such behavior. Mercimek et al. [41] conducted an experimental and numerical comparative study between three different strengthening methods to improve the flat slab punching behavior. The strengthening methods used shear studs, FRP, or textile-reinforced mortars (TRM) strips. The study concluded that using TRM was better compared to other methods. Mercimek et al. [42] investigated the punching shear performance of RC slabs with numerous openings in different locations of the two-way slabs. The slabs were strengthened using TRM strips with anchors. The results showed that the innovative strengthening method significantly enhanced the slabs' punching behavior. Türer et al. [43] studied the structural behavior of flat slabs with two openings near the column. The flat slabs were

strengthened against the punching failure using CFRP with fan-type anchors. The results showed that the strengthening technique increased the ultimate load capacity of the strengthened specimens by 50% on average compared with the unstrengthened control sample.

Yılmaz et al. [44] studied the structural behavior of RC two-way slabs subjected to low-velocity impact load. CFRP strips in different widths and orientations were used to strengthen the simply supported tested slabs. The results showed that using CFRP strips significantly enhanced the structural behavior of the tested specimens. The best results were obtained using wider CFRP strips in two diagonal orientations' directions. Al-Rousan et al. [45] studied the structural performance of RC slabs strengthened with different configurations and different layer numbers of the CFRP. The study concluded that using CFRP enhanced the flexural capacity and reduced the ductility of the strengthened specimens.

Many studies in the literature focused on the strengthening of the RC members by using the CFRP material. However, studies related to the effect of concrete compressive strength on the efficiency of strengthening the RC members by externally bonded CFRP are still relatively rare. In the current study, the examination of the impact of concrete compressive strength on the efficiency of using CFRP composite as the strengthened and repaired externally bonded material to improve the overall flexural capacity of RC two-way slabs is presented. Eight slabs are cast with low, normal, and high concrete compressive strength (i.e., 20, 35, 50, and 70) MPa, then strengthened or repaired with CFRP strips in the tension zone. The experimental evaluation of the flexural capacity, overall behavior, cracks pattern, and failure mode mechanism of the strengthened and repaired slabs are examined and discussed.

## 2. Experimental Study

**2.1. Properties of Materials.** To study experimentally the influence of varying concrete compressive strength on the flexural and overall behavior of RC two-way slabs strengthened and repaired with CFRP composite material, four different mixtures were designed to obtain a target of compressive strength with different values ranging from low to high strength (i.e., 20, 35, 50, and 70) MPa at 28 days. For all batches, cement type I was used; the physical properties of the cement used in this study that meet ASTM C150 [46] requirements are shown in Table 1. River sand and crushed dolomite with the maximum size of 5 and 25 mm for fine and coarse aggregate were used, respectively. Superplasticizer (Sika ViscoCrete-180 GS) was added to achieve the high compressive strength for all mixtures except for low strength mixture (C: 20). The proportions of concrete mixtures are summarized in Table 2.

For each batch, the strength of concrete was obtained from the average of three cubes with the size of 150 mm cast and tested according to BS EN 12390-3:2009 [47] while cylinders with the size of (150 × 300) mm were utilized to determine the splitting tensile strength according to ASTM C496M [48]. All the slabs, cubes, and cylinders were cast

TABLE 1: Physical properties of cement.

Physical properties	Test results	Limits of ASTM C150-04 [46]
Initial setting time (minutes)	115	$\geq 45$
Final setting time (minutes)	305	$\leq 375$
Fineness ( $m^2/kg$ )	315	$\geq 280$
Compressive strength (MPa)	14.7	$\geq 12$
3 days	23.4	$\geq 19$
7 days		
Specific gravity ( $g/cm^3$ )	3.15	—
Color	Light gray	—

TABLE 2: Proportions of concrete mixtures.

Concrete strength (MPa)	Materials' quantity ( $kg/m^3$ )				
	Cement	Fine aggregate	Coarse aggregate	Water	Superplasticizer
C: 20	300.0	782.5	1113.5	204.0	0.00
C: 35	402.0	723.5	1085.5	189.0	2.15
C: 50	447.0	710.5	1068.0	170.0	5.15
C: 70	548.0	674.0	1008.0	164.5	6.85

simultaneously and covered with wet burlap for several days, then after demolding, they were kept together under the same environmental condition in the same place until the examination day. The results of the mechanical properties of concrete and the internal reinforcement are provided in Table 3. All the information given for concrete in Table 3 was obtained at 28 days.

The proportion and distribution of the internal reinforcement were determined based on the ACI 318 code provision [49] to ensure all the slabs fail in flexural rather than punching shear. Based on that, the internal reinforcement grid consisted of five bars with the size of  $\Phi 12$  (dia. = 12.0 mm, area = 113 mm<sup>2</sup>), the spacing from center to center was 175 mm in both directions, and the reinforcement ratio  $\rho$  was 0.0095. This ratio was constant for all slabs, as illustrated in Figure 1. Three coupon samples were tested according to ASTM A370 [50] to obtain the internal reinforcement bar properties, and the results are summarized in Table 3. The experimental tests of the concrete and the steel reinforcement were conducted in the University of Basrah/Collage of Engineering laboratory.

**2.2. CFRP Composite.** For the strengthening system, the CFRP fabric material was SikaWrap-300C, as shown in Figure 2. The fabric is unidirectional woven fiber with a density of 1.82 g/cm<sup>3</sup>. To bond the carbon sheet to the concrete slab surface, an epoxy resin Sikadur-330 was utilized. This type of epoxy comprises two components, adhesive and thixotropic epoxy-based impregnating resin. The manufacturer's mechanical properties, as mentioned in the product data sheet of SikaWrap-300C and Sikadur-330, are provided in Table 4.

**2.3. Slabs' Description.** In the current work, eight RC two-way slabs were constructed and tested. All slabs had the same shape which is a square shape with dimensions of

(800 \* 800 \* 100) mm, as illustrated in Figure 3. The slabs were designed to fail in flexural and concrete clear cover was 20 mm based on ACI 318 code provision [49]. The slab designations are described in Table 5. Slabs were named differently based on the concrete strength. For slabs with concrete strength  $f'_c = 21.1$  MPa (C: 20), the control slab was named A-1, the strengthened slab A-2, and the repaired slab A-3. The same description was followed for the rest of the slabs except with changing the letter A to (B, C, and D) for slabs with concrete compressive strength (C35, C50, and C70), respectively.

Slabs were strengthened or repaired with one layer of CFRP strips in both directions on the tension face of the slab (lower face). The strip's width was 50 mm with a clear spacing between each strip was 150 mm; this arrangement was adopted according to the previous studies [44, 51] and as illustrated in Figure 3. The control slabs were repaired after testing with the same configuration as in the strengthened slabs.

**2.4. Specimens' Preparation.** The slab tension surface was roughened with a grinder, then the surface was cleaned with an air blower from any dirt and dust to ensure perfect bond characteristics between the concrete substrate and CFRP composite system. Marked all the strips' positions to make sure that all the strips were installed in the right place. The carbon fabric strips were cut into the desired length and width of 700 and 50 mm, respectively. The components of the epoxy agent resin were mixed exactly as recommended in the datasheet, and then the resin was applied to the marked locations of the strips. The precut strips were applied over the epoxy and pressed into the resin with a special tool to make sure the fabric was embedded perfectly in the epoxy resin. After 7 days of curing as recommended, the strips were covered to paint the rest of the slab surface with white paint to mark the cracks clearly during the test. The above-mentioned procedure is depicted in Figure 4.

TABLE 3: The measured properties of concrete and steel reinforcement.

Material	Concrete				Steel-reinforcing bars Φ12
	C: 20	C: 35	C: 50	C: 70	
Compressive strength, MPa	21.1	36.1	48.2	68.5	
Splitting tensile strength, MPa	1.7	2.5	3.1	4.3	
Yield stress, MPa					551
Ultimate strength, MPa					640
Modulus of elasticity, GPa					200

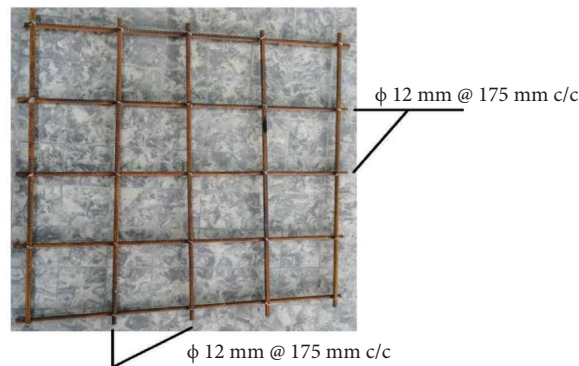


FIGURE 1: Internal reinforcement details.

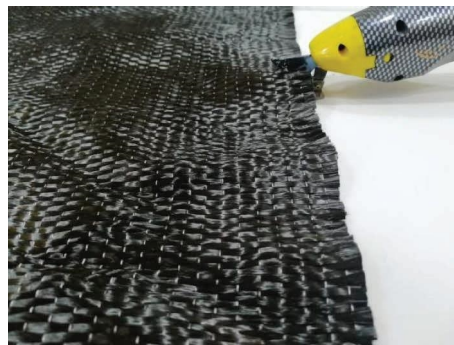


FIGURE 2: Carbon fabric.

TABLE 4: Mechanical properties of carbon fiber and epoxy resin.

Material	Tensile strength (MPa)	Modulus of elasticity (GPa)	Thickness (mm)	Elongation at break (%)
CFRP fabric	4000	230	0.167	1.7
Epoxy resin	30	4.5	—	0.9

For the repairing process, all the tenuous damaged parts and the cracks that took place on the top face (i.e., the compression side) of the control slabs during the test were sealed by adding Sikadur31 (epoxy paste adhesive). On the other hand, a new technique of repairing severely damaged parts and the wide cracks in the tension side is introduced. A repair material named Sikadur-52 LP was injected by using surface packers. To use this technique, all deep cracks in the tension zone surface were cleaned from any loose particles, dirt, and dust by using an air blower. Holes were made on the concrete tension surface exactly on the cracks track to install

surface packers which were situated at an approximate distance of 15 cm between each other. Then, the repair material (Sikadur-52 LP) was injected inside the cracks through surface packers. After a week, all surface packers were removed, followed by flattening the surface by using a grinder, and then the same procedure that had been done before with the strengthened slabs was followed. All the previous description of the repair process is shown in Figure 5. The manufacturer's properties as mentioned in the product datasheet of Sikadur-31 and Sikadur-52 LP at 7 days are given in Table 6.

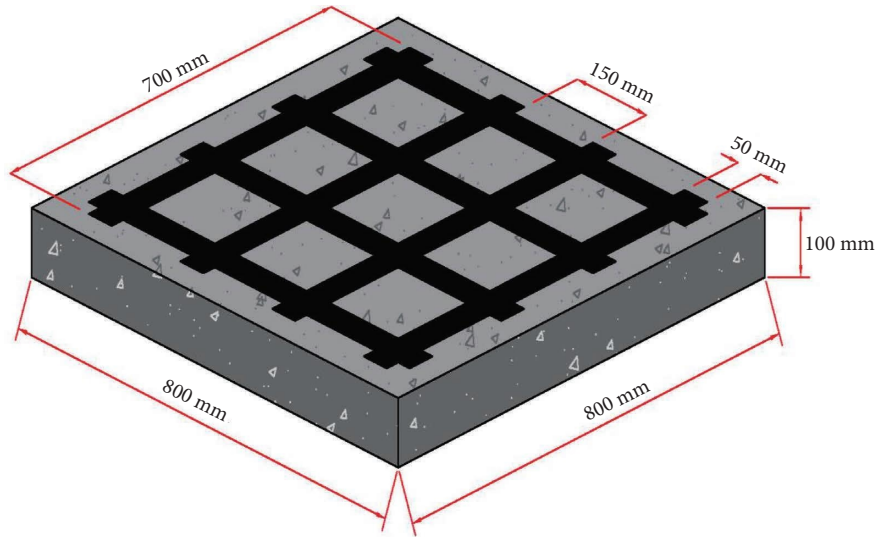


FIGURE 3: Slab dimensions.

TABLE 5: Slab designation.

Compressive strength, MPa	Slab description	Slab designation
C: 20	Control	A-1
	Strengthened	A-2
	Repaired	A-3
C: 35	Control	B-1
	Strengthened	B-2
	Repaired	B-3
C: 50	Control	C-1
	Strengthened	C-2
	Repaired	C-3
C: 70	Control	D-1
	Strengthened	D-2
	Repaired	D-3

**2.5. Test Set-Up and Instrumentation.** A universal testing machine, as depicted in Figure 6, was employed to apply a monotonic flexural loading on the specimens. The experimental test was performed under load control with increments of 5 kN/second, and the machine's maximum capacity was 2000 kN. To simulate the concept of simply supported reaction across all sides of the slabs, rigid square steel beams with side dimensions of 700 mm were utilized. Steel beams were implemented to ensure each slab would lay on a line of support with a distance of 50 mm from each edge. The load was directly imposed on the center of the slab by using a square steel plate with side dimensions of 200 mm. To measure the deflection beneath the center of the slab during the entire test duration, a laser dial gauge with an accuracy of 0.01 mm per division was installed. The test was paused each minute to examine, picture, and measure the crack width with a special tool, as shown in Figure 7. The test was stopped when the specimen exhibited incapacity to bear any additional load, compelling the necessity of terminating the examination.

### 3. Experimental Results and Discussion

**3.1. Overall Flexural Behavior.** The overall flexural behavior represented by the load-deflection curves is plotted in Figure 8 for all groups. The results were categorized into four groups depending on the concrete compressive strength values (i.e., C: 20, C: 35, C: 50, and C: 70). In general, the flexural behavior of the control slab in each group was similar and can be explained easily by dividing each curve into two distinct stages: the initial stage involved both the concrete and steel reinforcement behaving elastically and linearly until the first crack occurred in the concrete. During this stage, the slabs maintained high stiffness due to the absence of cracks. At this stage, the improvement in initial stiffness was 22.4, 26, 17.4, and 21.6%, respectively, for the slabs strengthened with CFRP strips, while the improvement was 6.2, 4.8, 3.3, and 9.9%, respectively, for the repaired slabs, as summarized in Table 7. The method for calculating the initial stiffness is shown in Figure 9 [11, 42] according to previous studies [12, 41, 44].

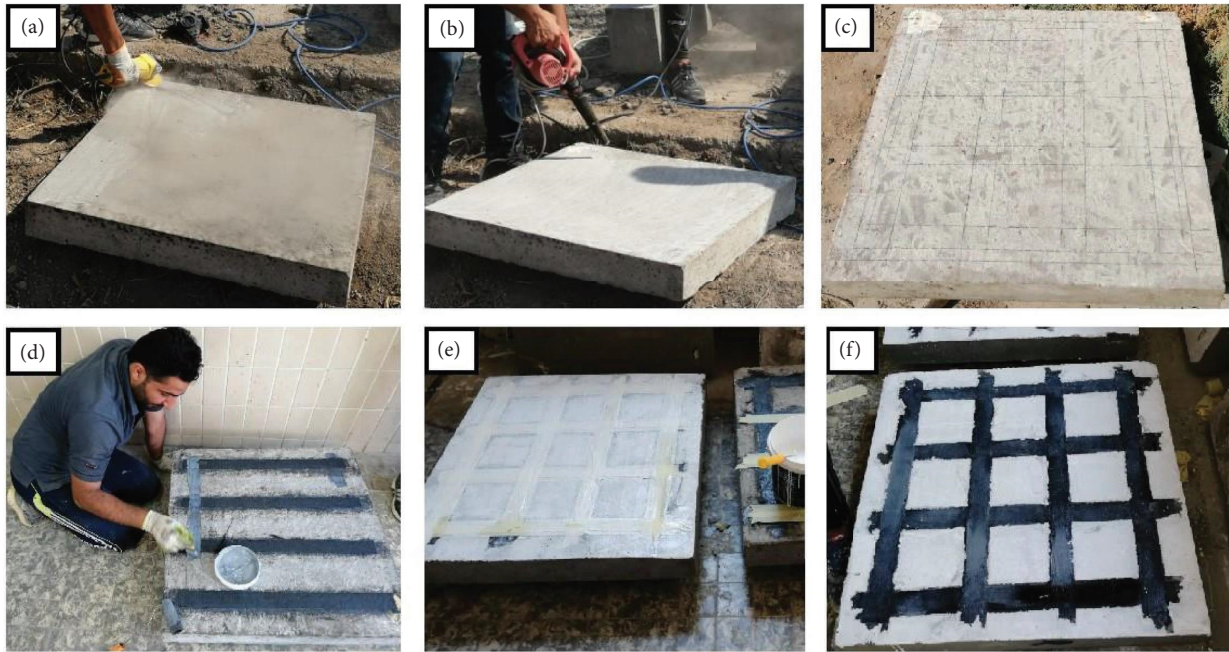


FIGURE 4: Strengthening installation procedure: (a) roughen the tension surface of the slab, (b) surface cleaning from any dirt or dust, (c) marking the composite position, (d) applying the epoxy agent followed by the carbon fabric, (e) covering the composite to paint the rest of the slab area, and (f) the final look of the specimen.



FIGURE 5: Repair process of control slabs after testing: (a) sealing the cracks on the compression side with Sikadur-31 material, (b) making holes and installing surface parkers on the tension side, (c) injecting Sikadur-52 LP material, (d) flattening the surface, (e) surface cleaning, and (f) applying the CFRP composite system.

TABLE 6: Mechanical properties of Sikadur-31 and Sikadur-52 LP.

Material	Tensile strength (MPa)	Modulus of elasticity (GPa)	Flexural strength (MPa)	Compressive strength (MPa)	Elongation at break (%)
Sikadur-31	22.7	10.3	42	85.5	0.9
Sikadur-52 LP	27	—	—	70	—

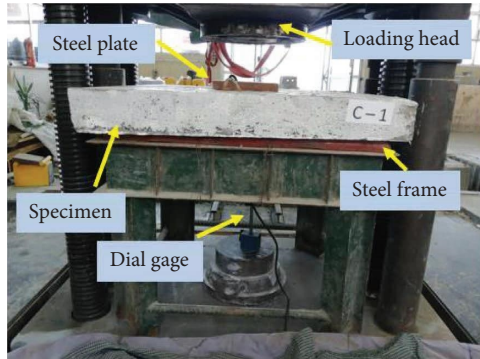


FIGURE 6: Test set-up and instrumentations.



FIGURE 7: Crack width measuring tool.

However, once the first crack appeared, there was a digression from the initial elastic response, indicating the onset of the second stage. In this subsequent stage, the nonlinear behavior became apparent due to the yielding of the steel reinforcement. As the cracks formed, the reduction in stiffness occurred owing to a dwindling in the cross-sectional area of the slab. Figure 8 clearly illustrates the reduction in stiffness for each slab. At this point, ductile behavior was observed as the internal reinforcement yielded progressively from the center of the slab towards the edges with increasing applied load. At the end of the second stage, the specimen is no longer able to carry any further load. Similar behavior was evident in both the strengthened and repaired slabs in comparison to control slabs. In Figure 8, the enhanced load capacity, conferred by the composite system, is visibly apparent when comparing the relevant slabs (A2 to A1, B2 to B1, C2 to C1, and D2 to D1). This contribution noticeably improved the overall behavior including the precracking stage by enhancing the stiffness and the ultimate capacity at the failure stage. However, in the case of the repaired slabs, the effectiveness of the composite system was not as remarkable as in the strengthened slabs. Likely, due to the damage of some parts during the test conducted on the

control slabs. The repaired system restored the original slab strength and added a slight improvement to the ultimate load capacity with extra ductile behavior before failure.

**3.2. Load-Carrying Capacity and Corresponding Deflection.** The test results represented by the applied load versus the corresponding deflection measured at the center of the slab are summarized in Table 7. The information in Table 7 includes the measurement values of cracking  $P_{cr}$  and failure  $P_F$  loads with the corresponding deflections (cracking  $\delta_{cr}$  and failure  $\delta_F$ ), respectively. The cracking load of control slabs was significantly affected by the concrete strength, which increased with the increment of compressive strength ( $f'c$ ) consequentially to the increase of the concrete tensile strength, as reported in Table 3. Furthermore, the other slabs, strengthened or repaired, also witnessed an enhancement in their cracking load, owing to the contribution of the composite system. These systems effectively arrest the creation and development of hairline cracks, thereby delaying the appearance of the first visible cracks. In addition, the slabs with high concrete strength of 70 MPa (i.e., D-series) experienced the most significant increase in cracking capacity, reaching up to 75.1% and 41.2% for the strengthened and repaired slabs (D2 and D3), respectively.

The ultimate loading capacity was related proportionally to the concrete strength. As the concrete strength increased, the slab's load capacity increased. The improvement was up to 23.3% compared to the control slab for slabs with the highest concrete strength (C: 70). On the other hand, the influence of the repairing system on the raising of the maximum loading capacity was approximately 7% compared to the control slab regardless to the concrete strength value.

The associated deflections to the cracking load were significantly lower than the control in strengthened slabs, while  $\delta_{cr}$  was the same or slightly higher in repaired slabs, as reported in Table 7. The inclusion of CFRP strips increased the cracking load magnitude by delaying the appearance of the first crack and, therefore, led to a higher value of stiffness at the cracking load which affected the deflection as well. Furthermore, the results in Table 7 reveal that the ductility at failure load  $\delta_F$  for repaired slabs was higher than the strengthened and control slabs since the repaired slabs had lower postcracking stiffness, whereas the CFRP composite system added more stiffness to the slabs by reducing the deflection with higher failure load.

**3.3. Crack Pattern and Mode of Failure.** The cracking pattern of tested slabs is depicted in Figure 10, and the failure mode is listed in Table 7. For the control slabs, the crack pattern was approximately the same for all groups. The first visible

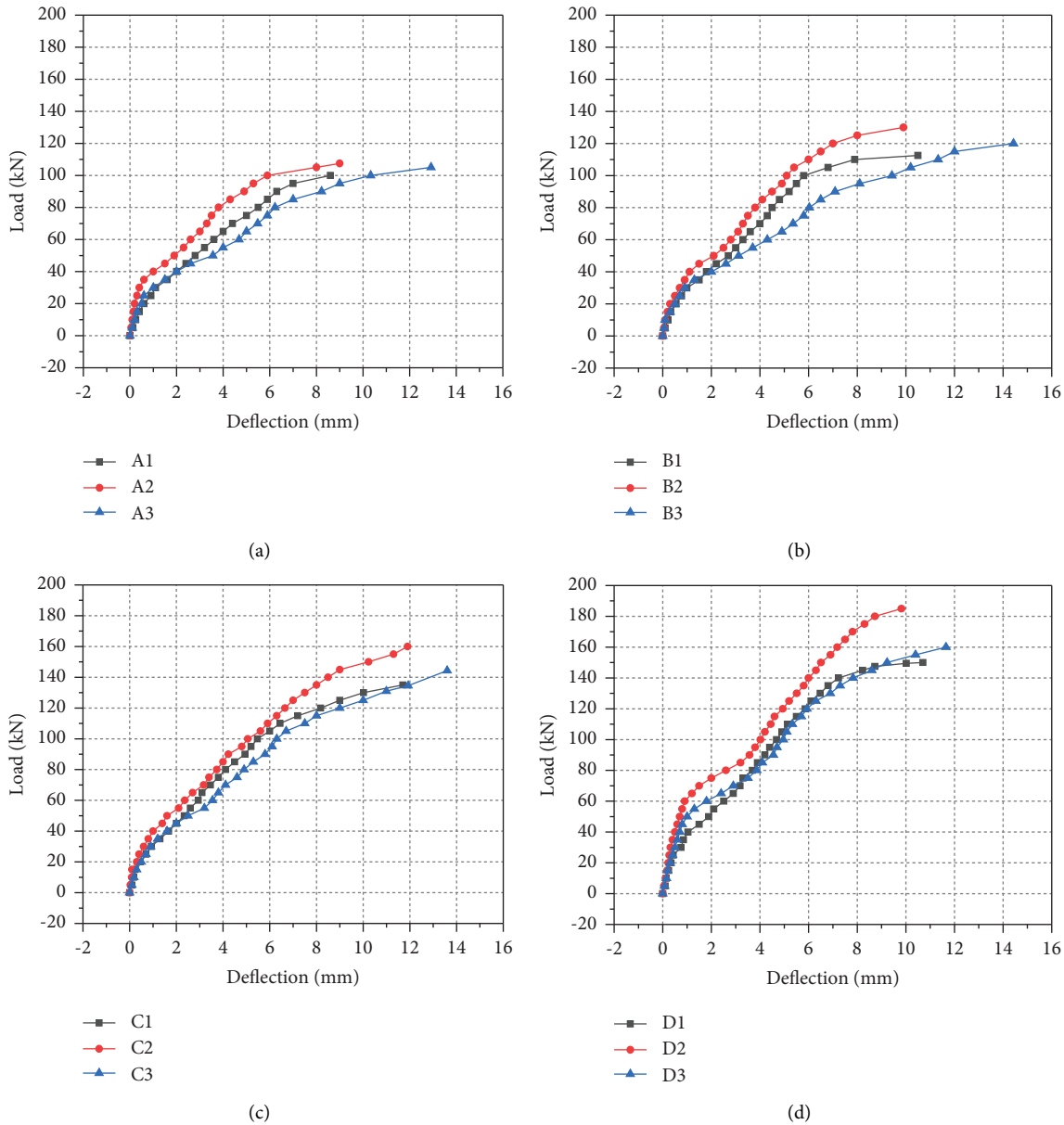


FIGURE 8: Load-deflection curves: (a) C: 20, (b) C: 35, (c) C: 50, and (d) C: 70.

crack initiated in the tension zone of the center of the slab, then more cracks appeared and propagated rapidly and diagonally towards the slab corners. It was observed that the width of the initial cracks was increased up to 2.5 mm as the load raised as shown in Figure 11(a). Flexural failure was observed indicated by the yielding of the internal reinforcement which was followed by minor damages in concrete in both tension and compression sides.

Slabs with low concrete strength (A-2 and A-3) had a similar cracking pattern as in A-1. The first visible crack formed in the middle of the slab tension side, followed by more cracks appearing in the zones between the strips as the load increased. The cracks stayed narrow up to 1.5 mm (Figure 11(b)) without widening because of the influence of CFRP composite on restraining the crack width. The failure was owing to the debonding of the CFRP strips from one of

the edges followed by minor damage in the concrete on both sides as in the control slab, A-1. Slabs with  $f'_c = 35$  MPa failed due to a combination of flexural and ductile punching shear for both strengthened and repaired slabs (i.e., B-2 and B-3), and the observation on the cracking patterns were the same as in A-2 and A-3, respectively. The crack width measured was 1.25 mm, as shown in Figure 11(c).

The failure mode of slabs in series C: 50 and C: 70 (i.e., C-2, C-3, and D-3) was ductile punching shear without any sign of flexural cracking on the tension side of the slab. This mode of failure mechanism was ductile punching shear failure due to the presence of the CFRP strips consolidated with the high strength of concrete which led to switching the failure from flexural to punching shear. The latest mode of failure is demonstrated in Figure 12. On the other hand, the failure of slab D-2 was due to debonding of the CFRP strips



TABLE 7: Summary of the experimental results.

Slab designation	Cracking load $P_{cr}$ (kN)	Percentage increased in cracking load (%)	Deflection at cracking load $\delta_{cr}$ (mm)	Failure load $P_F$ (kN)	Percentage increased in failure load (%)	Deflection at failure load $\delta_F$ (mm)	Energy dissipation (kN-mm)	Initial stiffness (kN/mm)	Failure mode
A1	21.0	—	0.60	100.0	—	8.6	564.0	32.20	Flexural failure CFRP debonding followed by flexural failure
A2	27.8	32.4	0.42	107.5	7.5	9.0	721.0	39.40	CFRP debonding followed by flexural failure
A3	26.5	26.2	0.58	105.0	5.0	12.9	944.0	34.20	Flexural failure
B1	26.0	—	0.77	112.5	—	10.5	812.0	33.50	Mixed between flexural and punching shear failure
B2	33.7	29.6	0.71	130.0	15.6	9.9	872.0	42.20	Mixed between flexural and punching shear failure
B3	31.5	21.2	0.81	120.0	6.7	14.4	1085.0	35.10	Mixed between flexural and punching shear failure
C1	28.8	—	0.90	135.0	—	11.7	998.0	36.70	Flexural failure
C2	37.6	30.6	0.83	160.0	18.5	11.9	1104.0	43.10	Punching shear failure
C3	34.0	18.1	0.98	145.0	7.4	15.9	1271.0	37.90	Punching shear failure
D1	35.4	—	0.96	150.0	—	10.7	1088.6	37.5	Flexural failure CFRP debonding followed by flexural failure
D2	62.0	75.1	0.91	185.0	23.3	9.8	1173.0	45.60	CFRP debonding followed by flexural failure
D3	50.0	41.2	1.02	160.0	6.7	11.7	1316.0	41.20	Punching shear failure

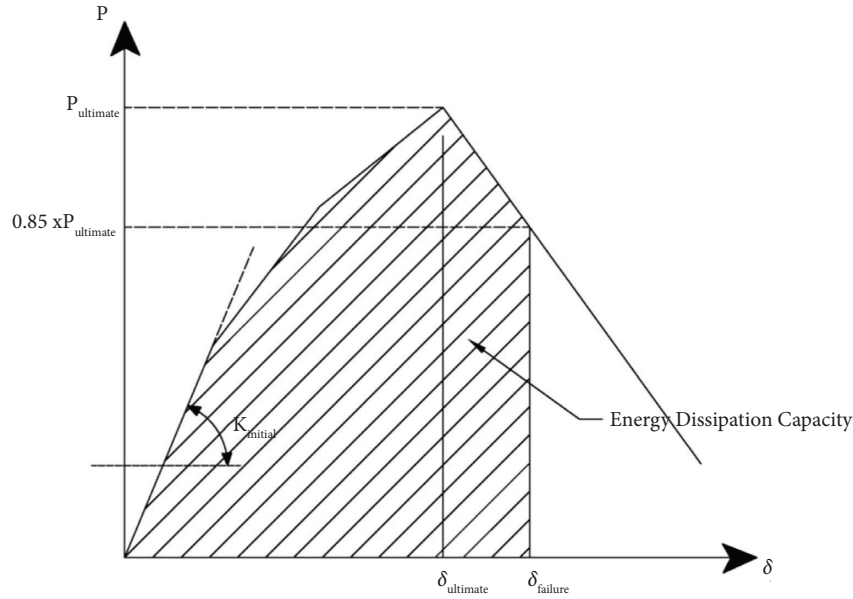


FIGURE 9: Method used to calculate initial stiffness and energy dissipation capabilities.

from one of the edges followed by minor damage in the tension and compression sides of the slab. It should be noted that all the cracks in the repaired slabs appeared in different locations than the old cracks' position of the control slab which indicated the power of the repairing technique.

**3.4. Energy Dissipation Capacity.** The energy dissipation capabilities were obtained by calculating the area under the load-displacement curve, where the energy dissipation capabilities of the tested samples were calculated up to the point of failure [11, 41, 44]. The method used to calculate the energy dissipation capabilities are shown in Figure 10 [52, 53].

The values of the energy dissipation capabilities of the control panels A1, B1, C1, and D1 were calculated, and the values were 654, 812, 998, and 1088.6 kN-mm, respectively, while the energy dissipation values for the slabs strengthened using CFRP strips A2, B2, C2, and D2 were 721, 872, 1104, and 1173 kN-mm, respectively. As for the repaired slabs A3, B3, C3, and D3, the values were 944, 1085, 1271, and 1316 kN-mm, respectively.

Thus, through the above values, it was observed that the strengthened slabs' samples improved by 27.8, 7.4, 10.6, and 7.8%, while the amount of improvement for the repaired slabs was 67.4, 33.6, 27.4, and 31.9%. Thus, the improvement average for the strengthened slabs was 13.4%, while the improvement average for the repaired slabs was 40.1%. Thus, although the value of increase in the repaired panels is greater than that in the strengthened slabs, this indicates that the repaired slabs were able to withstand a large amount of deflection despite the inability to bear any additional load.

#### 4. Analytical Study

The ultimate load capacity of the two-way reinforced concrete slab test specimens was calculated using the equations given in the regulations of [7, 28].

The flexural capacity of the control slabs can be estimated using the yield line theory. The method adopted in the current study is previously presented by Ebead and Marzouk and Akkaya et al. [7, 52]. This approach is based on the following equation:

$$P_{est.} = 8M_b \left( \frac{S}{L-c} - 0.172 \right), \quad (1)$$

where  $P_{est.}$  is the estimated load-carrying capacity based on the virtual work done by the action of the yield lines theory (kN),  $M_b$  is the radial moment capacity of the slab (N.mm/mm),  $S$  is the side length of the square slab (mm),  $L$  is the slab span (mm), and  $c$  is the length of the column side (mm).

The radial moment capacity  $M_b$  for the strengthened slab, however, is evaluated by adding the contribution of the strengthening materials. Therefore, the equation of  $M_b$  is consistence of two parts, as shown in the following equation:

$$M_b = M_{b1} + M_{b2}. \quad (2)$$

$M_{b1}$  is the unstrengthened capacity of the slab which is used alone to calculate the moments for control slabs and  $M_{b2}$  is the strengthened capacity of the slab.  $M_{b1}$  is evaluated according to the following equation:

$$M_{b1} = Ld^2 \rho f_y \left[ 1 - \frac{0.59 \rho f_y}{f'_c} \right], \quad (3)$$

where  $d$  is the distance from extreme compression fiber to centroid of tension reinforcement (mm),  $\rho$  is the tension reinforcement ratio of the slab,  $f_y$  is the yield stress of the slab reinforcement (MPa), and  $f'_c$  is the compressive strength of concrete (MPa).

While  $M_{b2}$  is evaluated according to the following expression, we assume full bonds between strengthening material and concrete:



FIGURE 10: Cracks' patterns and mode of failure.

$$M_{b2} = E_f t_f \varepsilon_f \left[ h - \frac{a}{2} \right] \frac{W_f}{\eta S}, \quad (4)$$

where  $E_f$  is the modulus of elasticity of FRP materials (MPa),  $t_f$  is the total thickness of FRP material (mm),  $\varepsilon_f$  is the strain in FRP strips' layer,  $h$  is the slab thickness (mm),

$a$  is the distance from the top of the slab to the neutral axis (mm),  $W_f$  is the width of FRP material (mm), and  $\eta$  is the effective strengthening width coefficient taken as 0.75 [7].

The strain in FRP  $\varepsilon_f$  and the depth of the neutral from the top of the slab  $a$  are calculated based on the following equations:

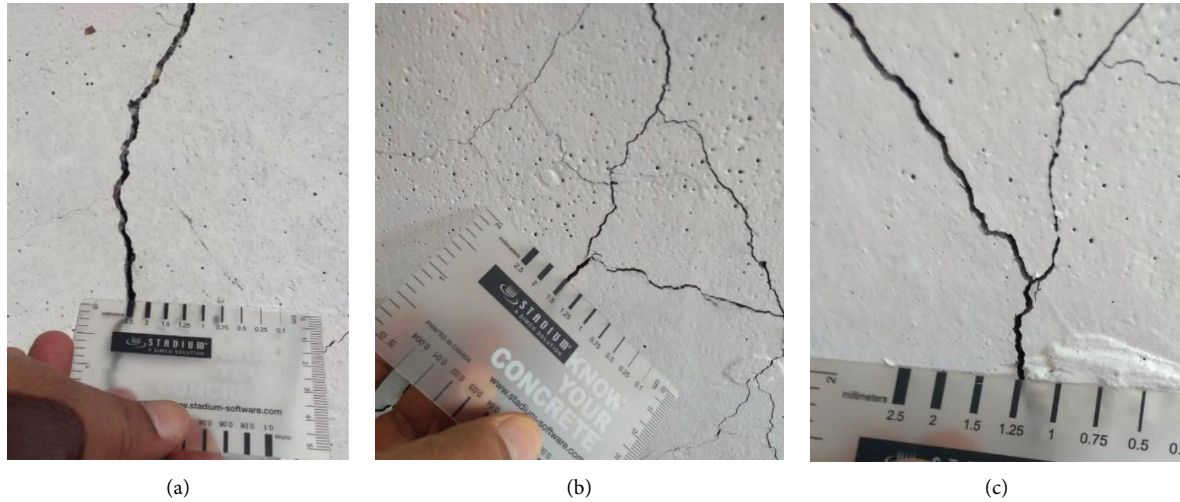


FIGURE 11: Measuring of crack width for (a) control, (b) series A, and (c) series B.



FIGURE 12: Punching shear failure.

TABLE 8: The compared values between the experimental ( $P_{exp}$ ) and estimated ( $P_{est}$ ) load capacity of the strengthened slabs.

Slab	$f'_c$ (MPa)	$P_{exp}$ ·kN	$P_{est}$ ·kN	$P_{exp}/P_{est}$
A1	21.1	100.0	99.8	1.00
A2	21.1	107.5	105.8	1.02
B1	36.1	112.5	109.4	1.03
B2	36.1	130.0	125.3	1.04
C1	48.2	135.0	129.2	1.04
C2	48.2	160.0	151.8	1.05
D1	68.5	150.0	141.1	1.06
D2	68.5	185.0	169.7	1.09

$$\varepsilon_f = \left[ \frac{h}{d} - 1 \right] \varepsilon_{cu} + \frac{h}{d} \varepsilon_y, \quad (5)$$

$$a = 0.8 \frac{d}{\varepsilon_{cu} + \varepsilon_y} \varepsilon_{cu}$$

where  $\varepsilon_y$  is the yield strain in steel reinforcement and  $\varepsilon_{cu}$  is the concrete failure strain in the extreme compressive fiber.

Furthermore, to evaluate the maximum load capacity of strengthened slab, the value of  $c$  in equation (1) should be

replaced by the width of the FRP strips  $W_f$ . Therefore, the following equation is used for strengthened slabs:

$$P_{est} = 8M_b \left( \frac{S}{L - W_f} - 0.172 \right). \quad (6)$$

The analytical evaluation of control and strengthened slabs are listed in Table 8 and plotted in Figures 13 and 14, respectively. The maximum load capacity of control slabs was estimated by using equation (1), while equation (6) was implemented for the strengthened slabs.

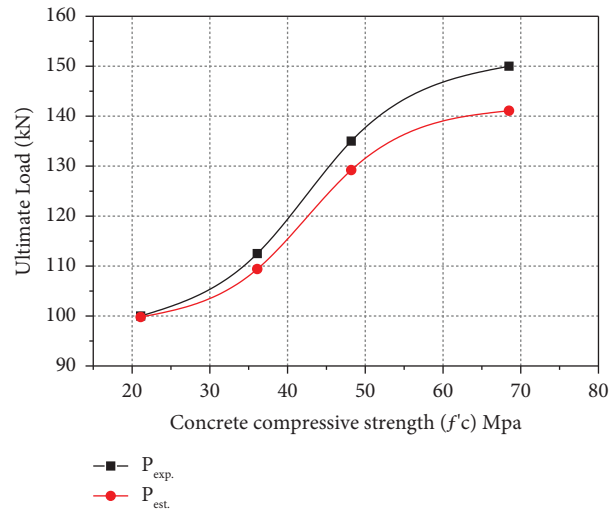


FIGURE 13: Comparison between the experimental and estimated maximum load capacity with the varying of the concrete compressive strength for control slabs.

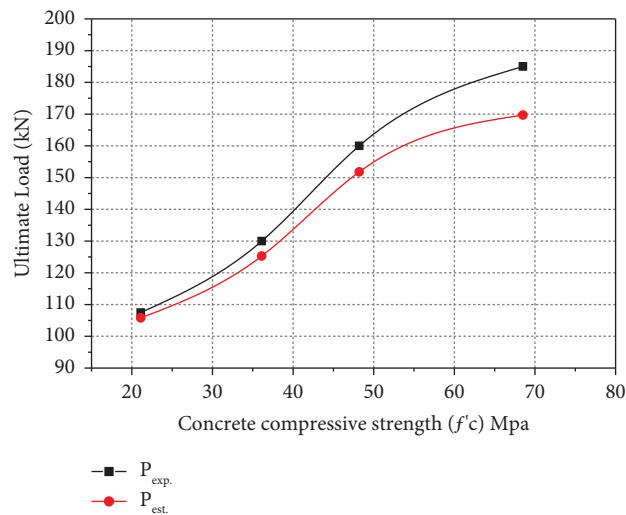


FIGURE 14: Comparison between the experimental and estimated maximum load capacity with the varying of the concrete compressive strength for strengthened slabs.

The method demonstrated good concordance with experimental data, achieving a margin of error under 10%, as shown in Table 7. Therefore, it is possible to use theoretical equations to estimate the ultimate load for control slabs and reinforced slabs.

It is notable that as the concrete compressive strength ( $f'_c$ ) increased, the divergence in the results between the estimated and experimental increased. This approach may not be accurate for high strength concrete. Therefore, more experimental investigations are required for slabs with compressive strength higher than 70 MPa.

## 5. Conclusions

In the present study, an experimental investigation of the influence of varying concrete compressive strength ( $f'_c$ ) on

the competence of using the CFRP as a strengthening and repairing system of RC two-way slabs on the load ultimate capacity, changes in stiffness, the overall behavior, and failure mechanism were introduced and examined. Eight RC two-way slabs were built with different concrete compressive strength ( $f'_c$ ) (i.e., 20, 35, 50, and 70) MPa and then either strengthened or repaired with one layer of CFRP strips. The slabs were examined experimentally under monotonic loading. The following considerable points were concluded:

- (1) The use of CFRP strips as a strengthening system significantly improved the behavior of the two-way RC slabs through an improvement in ultimate load, stiffness, and energy dissipation ability
- (2) The slabs with high compressive strength (D series) increased their ultimate capacity by 23.3% and 6.7%

for the strengthening and repairing systems, respectively, while the improvement in crack load was 75.1% and 41.2%, respectively

- (3) It was also noted that the ultimate load capacity was proportionally related to the strength of the concrete and increased with increasing concrete strength
- (4) For the slabs whose compressive strength was moderate,  $f_c = 35$  (series B), the failure was a combination of punching shear and flexural for both strengthened and repaired slabs, while the remaining specimens failed in shear without any sign of flexural cracking in the tension zone
- (5) The use of CFRP strips led to an improvement in the initial stiffness by an average of 21.8% and 6.0% for the strengthened and repaired slabs, respectively, while the improvement average in energy dissipation capabilities was 13.4% and 40.1% for the strengthened and repaired slabs, respectively
- (6) The theoretical results showed good agreement with the experimental results, and thus, it is possible to use theoretical equations to estimate the ultimate load for control slabs and strengthened slabs.

## Data Availability

All the data used to support the findings of this study are included within the manuscript.

## Additional Points

**Highlights.** (i) RC two-way slabs were either strengthened or repaired with one layer of CFRP composite strips and then tested experimentally under monotonic loading. (ii) The experimental evaluation of the flexural capacity, overall behavior, cracks pattern, and failure mode mechanism of the strengthened and repaired slabs were examined and discussed.

## Conflicts of Interest

The authors declare that they have no conflicts of interest.

## Acknowledgments

The study was self-funded by the researchers.

## References

- [1] G. De Schutter, *Damage to concrete Structures*, Taylor and Francis, Florida, NY, USA, 2013.
- [2] A. Abu-Obeidah, R. A. Hawileh, and J. A. Abdalla, "Finite element analysis of strengthened RC beams in shear with aluminum plates," *Computers and Structures*, vol. 147, pp. 36–46, 2015.
- [3] B. B. Adhikary, H. Mutsuyoshi, and M. Sano, "Shear strengthening of reinforced concrete beams using steel plates bonded on beam web: experiments and analysis," *Construction and Building Materials*, vol. 237, p. 244.
- [4] Ö Mercimek, R. Ghoroubi, A. Özdemir, Ö Anil, and Y., ar Erbas, "Investigation of strengthened low slenderness RC column by using textile reinforced mortar strip under axial load," *Engineering Structures*, vol. 259, Article ID 114191, 2022.
- [5] F. Pacheco-Torgal, R. E. Melchers, X. Shi, D. B. Nele, V. T. Kim, and S. Andres, *Eco-efficient Repair and Rehabilitation of concrete Infrastructures*, Elsevier, Amsterdam, The Netherlands, 2nd edition, 2024.
- [6] Y. D. Wang, S. Yang, M. Han, and X. Yang, "Experimental study of section enlargement with reinforced concrete to increase shear capacity for damaged reinforced concrete beams," *Applied Mechanics and Materials*, vol. 256–259, pp. 1148–1153, 2012.
- [7] U. Ebead and H. Marzouk, "Strengthening of two-way slabs using steel plates," *Structural Journal*, vol. 99, no. 1, pp. 23–31, 2002.
- [8] D. Banu and N. Taranu, "Traditional solutions for strengthening reinforced concrete slabs," *Buletinul Institutului Politehnic din Iasi. Sectia Constructii, Arhitectura*, vol. 56, no. 3, p. 53, 2010.
- [9] G. Foret and O. Limam, "Experimental and numerical analysis of RC two-way slabs strengthened with NSM CFRP rods," *Construction and Building Materials*, vol. 22, no. 10, pp. 2025–2030, 2008.
- [10] Y. J. Kim, J. M. Longworth, R. G. Wight, and M. F. Green, "Flexure of two-way slabs strengthened with prestressed or nonprestressed CFRP sheets," *Journal of Composites for Construction*, vol. 12, no. 4, pp. 366–374, 2008.
- [11] Ö. Mercimek, R. Ghoroubi, Ö. Anil, C. Çakmak, A. Özdemir, and Y. Kopraran, "Strength, ductility, and energy dissipation capacity of RC column strengthened with CFRP strip under axial load," *Mechanics Based Design of Structures and Machines*, vol. 51, no. 2, pp. 961–979, 2023.
- [12] R. Ghoroubi, O. Mercimek, A. Özdemir, and O. Anil, "Experimental investigation of damaged square short RC columns with low slenderness retrofitted by CFRP strips under axial load," *Structures*, vol. 28, pp. 170–180, 2020.
- [13] C. E. Bakis, L. C. Bank, V. Brown et al., "Fiber-reinforced polymer composites for construction State-of-the-art review," *Journal of Composites for Construction*, vol. 6, no. 2, pp. 73–87, 2002.
- [14] L. C. Bank, *Composites for Construction: Structural Design with FRP Materials*, John Wiley and Sons, Hoboken, NY, USA, 2006.
- [15] I. Shakir Abbood, S. a. Odaa, K. F. Hasan, and M. A. Jasim, "Properties evaluation of fiber reinforced polymers and their constituent materials used in structures—A review," *Materials Today: Proceedings*, vol. 43, pp. 1003–1008, 2021.
- [16] N. Haritos and A. Hira, "Repair and strengthening of RC flat slab bridges using CFRPs," *Composite Structures*, vol. 66, no. 1–4, pp. 555–562, 2004.
- [17] S. C. Floruș, V. Stoian, T. Nagy-György, D. Dan, and D. Diaconu, "Retrofitting of two-way RC slabs with and without cut-out openings by using FRP composite materials," in *Proceedings of the 3rd WSEAS International Conference on Engineering Mechanics, Structures, Engineering Geology (EMSESG'10)*, pp. 22–24, Cambridge, UK, July 2010.
- [18] A. Napoli, F. Matta, E. Martinelli, A. Nanni, and R. Realfonzo, "Modelling and verification of response of RC slabs strengthened in flexure with mechanically fastened FRP laminates," *Magazine of Concrete Research*, vol. 62, no. 8, pp. 593–605, 2010.
- [19] R. Al-Rousan, M. Issa, and H. Shabila, "Performance of reinforced concrete slabs strengthened with different types

- and configurations of CFRP,” *Composites Part B: Engineering*, vol. 43, no. 2, pp. 510–521, 2012.
- [20] J. Moon, M. M. Reda Taha, and J. J. Kim, “Flexural strengthening of RC slabs using a hybrid FRP-UHPC system including shear connector,” *Advances in Materials Science and Engineering*, vol. 2017, Article ID 4387545, 7 pages, 2017.
- [21] Z. R. Aljazeera and J. J. Myers, “Flexure performance of RC one-way slabs strengthened with composite materials,” *Journal of Materials in Civil Engineering*, vol. 30, no. 7, Article ID 04018120, 2018.
- [22] O. Al-Ghazawi and R. Z Al-Rousan, “Response of reinforced concrete slabs strengthened with CFRP,” *Journal of Engineering Science and Technology Review*, vol. 13, no. 6, pp. 125–129, 2020.
- [23] N. M. Ayash, A. M. Abd-Elrahman, and A. E. Soliman, “Repairing and strengthening of reinforced concrete cantilever slabs using Glass Fiber–Reinforced Polymer (GFRP) wraps,” *Structures*, vol. 28, pp. 2488–2506, 2020.
- [24] N. Moshiri, C. Czaderski, D. Mostofinejad et al., “Flexural strengthening of RC slabs with nonprestressed and prestressed CFRP strips using EBROG method,” *Composites Part B: Engineering*, vol. 201, Article ID 108359, 2020.
- [25] M. Abas Golham and A. H. A. Al-Ahmed, “Behavior of GFRP reinforced concrete slabs with openings strengthened by CFRP strips,” *Results in Engineering*, vol. 18, Article ID 101033, 2023.
- [26] O. Limam, G. Foret, and A. Ehrlacher, “RC two-way slabs strengthened with CFRP strips: experimental study and a limit analysis approach,” *Composite Structures*, vol. 60, no. 4, pp. 467–471, 2003.
- [27] A. S. Mosallam and K. M. Mosalam, “Strengthening of two-way concrete slabs with FRP composite laminates,” *Construction and Building Materials*, vol. 17, no. 1, pp. 43–54, 2003.
- [28] U. Ebead and H. Marzouk, “Fiber-reinforced polymer strengthening of two-way slabs,” *Structural Journal*, vol. 101, no. 5, pp. 650–659, 2004.
- [29] O. Limam, V. T. Nguyen, and G. Foret, “Numerical and experimental analysis of two-way slabs strengthened with CFRP strips,” *Engineering Structures*, vol. 27, no. 6, pp. 841–845, 2005.
- [30] O. Enochsson, J. Lundqvist, B. Täljsten, P. Rusinowski, and T. Olofsson, “CFRP strengthened openings in two-way concrete slabs—An experimental and numerical study,” *Construction and Building Materials*, vol. 21, no. 4, pp. 810–826, 2007.
- [31] Z. F. Chen, L. L. Wan, S. Lee et al., “Evaluation of CFRP, GFRP and BFRP material systems for the strengthening of RC slabs,” *Journal of Reinforced Plastics and Composites*, vol. 27, no. 12, pp. 1233–1243, 2008.
- [32] W. E. Elsayed, U. A. Ebead, and K. W. Neale, “Mechanically fastened FRP-strengthened two-way concrete slabs with and without cutouts,” *Journal of Composites for Construction*, vol. 13, no. 3, pp. 198–207, 2009.
- [33] B. J. Al-Sulayvani and D. N. Al-Talabani, “Strengthening and repair of circular RC slabs with openings using CFRP strips under repeated loading,” *Construction and Building Materials*, vol. 84, pp. 73–83, 2015.
- [34] R. Khajehdehi and N. Panahshahi, “Effect of openings on in-plane structural behavior of reinforced concrete floor slabs,” *Journal of Building Engineering*, vol. 7, pp. 1–11, 2016.
- [35] M. Ravindra, V. Rakesh, and K. Rambabu, “A comparative study of strength of Two-Way rectangular slabs with and without openings,” *Journal-The Institution of Engineers: Series A*, vol. 98, no. 1-2, pp. 1–14, 2017.
- [36] T. Yılmaz, N. Kırac, Ö. Anil, R. T. Erdem, and C. Sezer, “Low-velocity impact behaviour of two-way RC slab strengthening with CFRP strips,” *Construction and Building Materials*, vol. 186, pp. 1046–1063, 2018.
- [37] M. Dewan and M. D. Abdulla, “Flexural behavior of RC two-way slabs with opening strengthened with CFRP sheets,” *Muthanna Journal of Engineering and Technology (MJET)*, vol. 6, no. 2, pp. 200–209, 2018.
- [38] A. Eskandarinadaf and M. Reza Esfahani, “Strengthening of two-way RC slabs with central opening,” *KSCE Journal of Civil Engineering*, vol. 23, no. 3, pp. 1228–1235, 2019.
- [39] M. J. Hussein, H. A. Jabir, and T. S. Al-Gasham, “Retrofitting of reinforced concrete flat slabs with cut-out edge opening,” *Case Studies in Construction Materials*, vol. 14, 2021.
- [40] M. K. Medhloom and E. N. Abed, “Behavior and load capacity of concrete slab reinforced by CFRP bar and strengthening by CFRP laminates,” *Civil and Environmental Engineering*, vol. 19, no. 1, pp. 72–85, 2023.
- [41] O. Mercimek, R. Ghoroubi, Y. Erbaş, and Ö. Anil, “Comparison of strengthening methods to improve punching behavior of two-way RC flat slabs,” *Structures*, vol. 46, pp. 1495–1516, 2022.
- [42] Ö. Mercimek, R. Ghoroubi, A. Özdemir, Ö. Anil, and M. Baran, “Punching behaviour of two-way RC slabs having different multiple opening locations and sizes strengthened with TRM,” *Structures*, vol. 42, pp. 531–549, 2022.
- [43] A. Türer, Ö. Mercimek, Ö. Anil, and Y. Erbas, “Experimental and numerical investigation of punching behavior of two-way RC slab with different opening locations and sizes strengthened with CFRP strip,” *Structures*, vol. 49, pp. 918–942, 2023.
- [44] T. Yılmaz, N. Kırac, Ö. Anil, R. T. Erdem, and C. Sezer, “Low-velocity impact behaviour of two way RC slab strengthening with CFRP strips,” *Construction and Building Materials*, vol. 186, pp. 1046–1063, 2018.
- [45] R. Al-Rousan, M. Issa, and H. Shabila, “Performance of reinforced concrete slabs strengthened with different types and configurations of CFRP,” *Composites Part B: Engineering*, vol. 43, no. 2, pp. 510–521, 2012.
- [46] Astm, *Standard Specification for Portland Cement*, ASTM International, West Conshohocken, PA, USA, 2004.
- [47] B. En, “Testing hardened concrete,” *Compressive Strength of Test Specimens*, vol. 12, 2009.
- [48] Astm, *Standard Test Method for Splitting Tensile Strength of Cylindrical concrete Specimens*, ASTM International, West Conshohocken, PA, USA, 2011.
- [49] Aci, *Building Code Requirements for Structural concrete (318M-14) and Commentary (318R-14)*, American Concrete Institute, Farmington Hills, MI, USA, 2014.
- [50] Astm, *Standard Test Methods and Definitions for Mechanical Testing of Steel Products*, ASTM International, West Conshohocken, PA, USA, 2016.

- [51] J. Radnic, D. Matešan, N. Grgic, and G. Baloevic, "Impact testing of RC slabs strengthened with CFRP strips," *Composite Structures*, vol. 121, pp. 90–103, 2015.
- [52] S. T. Akkaya, Ö. Mercimek, R. Ghoroubi, Ö. Anil, Y. Erbaş, and T. Yılmaz, "Experimental, analytical, and numerical investigation of punching behaviour of two-way rc slab with multiple openings," *Structures*, vol. 43, pp. 574–593, 2022.
- [53] A. Türer, Ö. Mercimek, Ö. Anil, and Y. Erbaş, "Experimental and numerical investigation of punching behavior of two-way RC slab with different opening locations and sizes strengthened with CFRP strip," *Structures*, vol. 49, pp. 918–942, 2023.